ISSN (Online) 2456 -1304

International Journal of Science, Engineering and Management (IJSEM)
Vol 2, Issue 6, June 2017

Laminar flow of electrically conducting non-Newtonian power – law fluid past a stretching flat surface in the presence of thermal dispersion using spectral relaxation method

[1] Uma maheswara rao K, [2] G.Koteswara rao
[1]Department of Mathematics
[1] Hyderabad Institute of Technology and management, Gowdavelly village, Rangareddy district, Hyderabad, Telangana 501401
[2] Department of Mathematics, Acharya Nagarjuna University,Guntur522510

Abstract: **In this present study, a numerical investigation has been carried out to discuss the steady, two dimensional laminar flow of heat and mass transfer of electrically conducting non-Newtonian power law fluid in the presence of thermal dispersion. The flow is induced by a stretching flat surface. The solutions of the transformed nonlinear equations have been obtained by using Spectral Relaxation Method (SRM) and the results are validated by comparison with numerical approximations obtained using the Matlab in-built boundary value problem solver bvp4c, and with existing results available in literature. The results are presented graphically and discussed for various resulting parameters. The rate of heat and mass transfer become larger for shear thinning fluids compared to Newtonian fluid and shear thickening fluids. Thermal dispersion strongly influenced the temperature profile.**

Keywords: Stretching flat sheet, non-Newtonian power law fluid, thermal dispersion, SRM.

I. INTRODUCTION

Investigations of boundary layer flow and heat transfer of viscous fluids over a flat sheet are important in many manufacturing processes, such as polymer extrusion, drawing of copper wires, continuous stretching of plastic films and artificial fibers, hot rolling, wire drawing, glass-fiber, metal extrusion, and metal spinning. Among these studies, Sakiadis [1] initiated the study of the boundary layer flow over a stretched surface moving with a constant velocity and formulated a boundary-layer equation for two-dimensional and axisymmetric flows. Tsou et al. [2] analyzed the effect of heat transfer in the boundary layer on a continuous moving surface with a constant velocity and experimentally confirmed the numerical results of Sakiadis [1]. Erickson et al. [3] extended the work of Sakiadis [1] to include blowing or suction at the stretched sheet surface on a continuous solid surface under constant speed and investigated its effects on the heat and mass transfer in the boundary layer. Ishak [4] investigated the heat transfer analysis for a mocropolar fluid over a stretching sheet with thermal radiation effect using Runge – Kutta – Fehlberg method. In another study, Ishak et al. [5] have been numerically investigated the unsteady boundary layer flow of heat transfer over a stretching vertical surface.

Many industrial fluids such as particulate slurries (china clay and coal in water, sewage sludge, etc.), multi-phase mixtures (oil-water emulsions, gas-liquid dispersions, froths and foams, butter), pharmaceutical formulations, cosmetics and toiletries, paints, synthetic lubricants, biological fluids (blood, synovial fluid, salvia), and foodstuffs (jams, jellies, soups, marmalades) in their flow characteristics can be sorted into the non-Newtonian fluids. These kinds of fluids possess two distinguishable properties. One is that their viscosity obeys a relation analogous to the Hookian relation between a stress and its strain, i.e. the stress is proportional to the strain rate. The other is that their Reynolds number and Grashof number are low owing to their large apparent viscosities. In engineering practice, the laminar flows of non-Newtonian fluids are encountered more common than those Newtonian fluid flows. Among those most popular models for the explanation of the non-Newtonian behavior of fluids, the empirical Ostwaald-de Waele model (or the power-law model) gains much acceptance due to its apparent simplicity in mathematics and its adequate description of many non-

ISSN (Online) 2456 -1304

International Journal of Science, Engineering and Management (IJSEM)
Vol 2, Issue 6, June 2017

Newtonian fluids over the most important range of shear rates. Studies of non-Newtonian fluids flow over moving sheets have been received considerable attention in the past decades due to their important applications in engineering and science. Among these works, the theoretical analysis of boundary layer equations for non-Newtonian power-law fluids was first performed by Schowalter [6] and Acrivos et al. [7]. Xu and Liao [8] investigated the laminar boundary layer flow of non-Newtonian fluids and heat transfer through a stretching flat sheet. They were considered both shear thinning fluids and shear thickening fluids. Hassanien et al [9] have been investigated the heat transfer analysis and flow configuration in a non-Newtonian power law fluid past a non-isothermal stretching sheet. Mohmoud and Megahed [10] studied the effects of non-uniform heat generation and heat transfer on a non-Newtonian power law fluid past a non-linearly stretching sheet. In another study Mohmoud and Megahed [11] have been investigated the effects of viscous dissipation and heat generation (absorption) on thermal boundary layer flow of a non-Newtonian fluid past a continuously moving permeable flat plate. Javed et al [12] have been numerically investigated the boundary layer flow of a non-Newtonian Eyring-Powel non – Newtonian fluid past a stretching sheet using Keller box method. Abd elmaboud and Mekheimer [13] investigated the non-Newtonian effects on peristaltic transport of a second order fluid through a porous medium.

Magnetohydrodynamic (MHD) is the science which deals with the motion of a highly conducting fluids in the presence of a magnetic field. The motion of the conducting fluid across the magnetic field generates electric currents which change the magnetic field, and the action of the magnetic field on these currents gives rise to mechanical forces which modify the flow of the fluid [14]. Mixed convective boundary layer flow of electrically conducting non-Newtonian power law fluid and heat transfer analysis over a vertical stretching sheet was studied by Prasad et al.[15]. They were concluded that the local Nusselt number and local Sherwood number decreases as the magnetic field increases. Effects of suction or injection, viscous dissipation on electrically conducting non-Newtonian power law fluid over a continuously moving porous flat plate with heat flux have been studied by Kavitha and Kishan [16]. Chen [17] studied the electrically conducting non-Newtonian power law fluids over a power law stretched sheet with heat flux in addition suction/injection. Convective boundary layer flow of a heat and mass transfer in an electrically conducting power law fluid past a heated vertical porous plate was investigated by Olajuwon [18]. Mekheimer et al. [19] studied the viscous, compressible and electrically conducting Maxwell fluid transport induced by a surface acoustic wave in a micro channel with slip effect. The effect of induced magnetic field on peristaltic transport of a micropolar fluid in a symmetric channel is investigated by Mekheimer [20]. He concluded that axial – induced magnetic field is higher for a Newtonian than that for a micropolar fluid and smaller as the transverse magnetic field increases. Mekheimer et al. [21] have been studied the induced magnetic field on blood flow through an anisotropically tapered elastic artery with overlapping stenosis in an anuulus. Mehkeimer and Al-Arabi [22] studied the peristaltic transport of magnetohydrodynamic flow through a homogenious porous medium in a planner channel. Gangadhar and Bhaskar Reddy [23] have been numerically investigated the MHD flow over a moving vertical plate.

The above cited articles in the literature explicates the flow and the heat and mass transfer characteristics of different working fluids in stretching sheet It can be noticed that consideration non-Newtonian power-law fluid as working fluid has greater interest in practical applications in science and engineering. As a trial attempt, the authors intend to provide the knowledge of the effects of the steady, two dimensional laminar flow of heat and mass transfer of magnetic non-Newtonian power-law fluid over a stretching flat sheet in the presence of thermal dispersion.

II. MATHEMATICAL FORMULATION

Consider the problem of two-dimensional laminar flow of steady incompressible and electrically conducting, viscous non-Newtonian power – law fluid over a wall coinciding with plane $y = 0$, the flow is being confined to $y > 0$. the flow is generated due to the linear stretching sheet. It is considered that the sheet moves with a velocity considering to a power – law from, i.e. $U_w = Cx^m$, and is subject to a prescribed surface temperature and concentration, that is $T_w = T_\infty + Ax^r \;\&\; C_w = C_\infty + Ax^r$.

The external force f may be written as follows:

$$f = J \times B \qquad (1)$$

where $J = \sigma_0 (E + V \times B)$ is the current density and $B = (0, B_0)$ is the transverse uniform magnetic field applied to the fluid layer. The symbols σ_0 and E are the

ISSN (Online) 2456 -1304

International Journal of Science, Engineering and Management (IJSEM)
Vol 2, Issue 6, June 2017

electric conductivity and the electric field, respectively. The external electric field is assumed to be zero and under the condition that magnetic Reynolds number is small the induced magnetic field is negligible compared with the applied field. Accordingly, the Hall effect is neglected.

The continuity, momentum, energy and species equations for the non-Newtonian power-law fluid after applying the boundary layer approximations can be expressed as:

$$\frac{\partial u}{\partial x}+\frac{\partial v}{\partial y}=0 \qquad (2)$$

$$u\frac{\partial u}{\partial x}+v\frac{\partial u}{\partial y}=\frac{1}{\rho}\frac{\partial \tau_{xy}}{\partial y}-\frac{\sigma B_0^2}{\rho}u \qquad (3)$$

$$u\frac{\partial T}{\partial x}+v\frac{\partial T}{\partial y}=\frac{\partial}{\partial y}\left(\alpha_e\frac{\partial T}{\partial y}\right) \qquad (4)$$

$$u\frac{\partial C}{\partial x}+v\frac{\partial C}{\partial y}=D\frac{\partial^2 C}{\partial y^2} \qquad (5)$$

Boundary conditions are

$$u(x,0)=U_w=Cx^m, v(x,0)=0, T(x,0)=T_\infty+Ax^r, C(x,0)=C_\infty+Ax^r \qquad (6)$$

$$y\to\infty: u\to 0, T\to T_\infty, C\to C_\infty \qquad (7)$$

Where ρ is the density of the fluid, α is the thermal conductivity of the fluid, D is the mass diffusivity of the fluid, the shear stress tensor is defined by the Ostwaldde – Wäle model, see Andersson et al. [24] or Liao [25],

$$\tau_{ij}=2K(2D_{kl}D_{kl})^{(n-1)/2}D_{ij} \qquad (8)$$

In which

$$D_{ij}=\frac{1}{2}\left(\frac{\partial u_i}{\partial x_j}+\frac{\partial u_j}{\partial x_i}\right) \qquad (9)$$

Therefore the momentum equation (3) is written as

$$u\frac{\partial u}{\partial x}+v\frac{\partial u}{\partial y}=-\frac{K}{\rho}\frac{\partial}{\partial y}\left(-\frac{\partial u}{\partial y}\right)^n-\frac{\sigma B_0^2}{\rho}u \qquad (10)$$

We are interested in similarity solution of the above boundary value problem; therefore, we introduce the following similarity transformations

$$\eta=\frac{y}{x}\left(\mathrm{Re}_x\right)^{1/(n+1)}, \psi(x,y)=U_w x\left(\mathrm{Re}_x\right)^{-1/(n+1)}, \quad \theta(\eta)=\frac{T-T_\infty}{T_w-T_\infty}, \varphi(\eta)=\frac{C-C_\infty}{C_w-C_\infty} \qquad (11)$$

Where $\psi(x,y)$ is the stream function which defines in usual way by $u=\frac{\partial\psi}{\partial y}$ & $v=-\frac{\partial\psi}{\partial x}$.

Making use of transformations (14), Equations (3)-(10) take the form

$$n(-f'')^{n-1}f'''+\frac{2mn-m+1}{n+1}ff''-mf'^2-Mf'=0 \qquad (12)$$

$$\theta''(1+Dsf')+Ds\theta' f''+\Pr\frac{2mn-m+1}{n+1}f\theta'-r\Pr f'\theta=0 \qquad (13)$$

$$\phi''+Sc\frac{2mn-m+1}{n+1}f\phi'-rScf'\phi=0 \qquad (14)$$

the transformed boundary conditions

$$f(0)=0, f'(0)=1, \theta(0)=1, \phi(0)=1 \qquad (15)$$

$$f'(\infty)=0, \theta(\infty)=0, \phi(\infty)=0 \qquad (16)$$

The non-dimensional constants in Equations (12)-(14) are the Reynolds number Re_x, the Prandtl number $\Pr$, magnetic parameterr M, thermal dispersion parameter Ds and the Schmidt number Sc. They are, respectively, defined as:

$$\mathrm{Re}_x=\frac{\rho x^m U_w^{2-n}}{K}, \Pr=\frac{U_w x}{\alpha}\mathrm{Re}_x^{-2/(n+1)}, \quad M=\frac{\sigma B_0^2}{\rho C}, Ds=\frac{\gamma du_w}{\alpha_m}, Sc=\frac{U_w x}{D}\mathrm{Re}_x^{-2/(n+1)} \qquad (17)$$

To seek the global similarity solutions for this flow problem, we expand the generalized Prandtl number *Pr* and Schmidt number *Sc* in the following form

ISSN (Online) 2456 -1304

International Journal of Science, Engineering and Management (IJSEM)
Vol 2, Issue 6, June 2017

$$\Pr = \frac{U_w x}{\alpha}\mathrm{Re}_x^{-2/(n+1)} = C^{\frac{3(n-1)}{n+1}}(K/\rho)^{\frac{2}{n+1}}x^{\frac{(3m-1)(n-1)}{n+1}}/\alpha$$
$$Sc = \frac{U_w x}{D}\mathrm{Re}_x^{-2/(n+1)} = C^{\frac{3(n-1)}{n+1}}(K/\rho)^{\frac{2}{n+1}}x^{\frac{(3m-1)(n-1)}{n+1}}/D \quad (18)$$

It is shown in the above equation that, when $n=1$ or $m=1/3$, the Prandtl number and Schmidt numbers no larger contain x term such that equations (12)-(14) admit the global similarity solutions. For the case $n=1$, equations (12)-(14) become the classical equations describing the boundary layer flow, heat and mass transfer of a Newtonian fluid through a stretching flat sheet. Although for the case $m=1/3$, the global similarity solutions are in existence for all types of fluids, that is the shear-thinning fluids $(n<1)$, shear-thickening fluids $(n>1)$, and the Newtonian fluid $(n=1)$.

These parameters, respectively, characterize the surface drag, wall heat and mass transfer rates. The shearing stress of the non – Newtonian power - law fluid at the surface of the wall τ_w is given by:

$$\tau_w = \left[K\left|\frac{\partial u}{\partial y}\right|^{n-1}\frac{\partial u}{\partial y}\right]_{y=0} \quad (19)$$

where μ is the coefficient of viscosity. The skin friction coefficient is defined as:

$$C_f = \frac{\tau_w}{\rho U_w^2/2} = 2\,\mathrm{Re}_x^{-1/(n+1)}\left|f''(0)\right|^{n-1}f''(0) \quad (20)$$

The heat transfer rate at the surface flux at the wall is given by:

$$q_w = -k\left(\frac{\partial T}{\partial y}\right)_{y=0} \quad (21)$$

where k is the thermal conductivity of the nanofluid. The Nusselt number is defined as:

$$Nu_x = \frac{x}{k}\frac{q_w}{T_w - T_\infty} \quad (22)$$

Using Equation (21) in (22) the dimensionless wall heat transfer rate is obtained as below:

$$\frac{Nu_x}{\mathrm{Re}_x^{1/(n+1)}} = -\theta'(0) \quad (23)$$

The mass flux at the surface of the wall is given by:

$$J_w = -D\left(\frac{\partial C}{\partial y}\right)_{y=0} \quad (24)$$

and the Sherwood is defined as:

$$Sh_x = \frac{x}{D}\frac{J_w}{C_w - C_\infty} \quad (25)$$

Using Equation (24) in (25) the dimensionless wall mass transfer rate is obtained as:

$$\frac{Sh_x}{\mathrm{Re}_x^{1/(n+1)}} = -\phi'(0) \quad (26)$$

Solution of the Problem:

In order to solve the equations (12)-(14) subject to the boundary conditions (15) and (16) the Spectral Relaxation Method (SRM) suggested by Motsa and Makukula [26] and Kameswaran et al. [27] is used. The method uses the Gauss- Seidel approach to decouple the system of equations. In the framework of SRM method the iteration scheme is obtained as

$$f'_{r+1} = p_{r+1},\ f_{r+1}(0) = 0 \quad \ldots(27)$$

$$p''_{r+1}\left(n\left(-p'_{r+1}\right)^{n-1}\right) + \left(\frac{2mn-m+1}{n+1}\right)f_{f+1}p'_{r+1} - Mp_{r+1} = mp_{r+1}^2 \quad \ldots.(28)$$

$$\theta''_{r+1}(1+Dsp_{r+1}) + \left(Dsp'_{r+1} + \Pr\left(\frac{2mn-m+1}{n+1}\right)f_{r+1}\right)\theta'_{r+1} - r\Pr\, p_{r+1}\theta_{r+1} = 0 \quad \ldots;(29)$$

$$\phi''_{r+1} + Sc\left(\left(\frac{2mn-m+1}{n+1}\right)f_{r+1}\right)\phi'_{r+1} - rScp_{r+1}\phi_{r+1} = 0 \quad \ldots(30)$$

The boundary conditions for the above iteration scheme are

$$p_{r+1}(0) = 1, \theta_{r+1}(0) = 1, \phi_{r+1}(0) = 1 \quad (31)$$

$$p_{r+1}(\infty) = 0, \theta_{r+1}(\infty) = 0, \phi_{r+1}(\infty) = 0 \quad (32)$$

In order to solve the decoupled equations (27) - (30), we use the Chebyshev spectral collocation method. The computational domain [0, L] is transformed to the

ISSN (Online) 2456 -1304

International Journal of Science, Engineering and Management (IJSEM)
Vol 2, Issue 6, June 2017

interval [-1, 1] using $\eta = L(\xi+1)/2$ on which the spectral method is implemented. Here L is used to invoke the boundary conditions at ∞. The basic idea behind the spectral collocation method is the introduction of a differentiation matrix $\mathcal{D}$ which is used to approximate the derivatives of the unknown variables at the collocation points as the matrix vector product of the form

$$\frac{\partial f_{r+1}}{\partial \eta} = \sum_{k=0}^{\bar{N}} D_{lk} f_r(\xi_k) = Df_r, l = 0,1,2,.....\bar{N} \quad (33)$$

where $\bar{N}+1$ is the number of collocation points (grid points), D = 2$\mathcal{D}$/L, and $f = \left[f(\xi_0), f(\xi_1), f(\xi_2),.....f(\xi_{\bar{N}})\right]^T$ is the vector function at the collocation points. Higher-order derivatives are obtained as powers of D, that is,

$$f_r^{(p)} = D^p f_r \quad (34)$$

where p is the order of the derivative. Applying the spectral method to equations (27)- (30), we obtain

$$A_1 f_{r+1} = B_1,\ f_{r+1}(\xi_{\bar{N}}) = 0 \quad (35)$$

$$A_2 p_{r+1} = B_2,\ p_{r+1}(\xi_{\bar{N}}) = 1,\ p_{r+1}(\xi_0) = 0 \quad (36)$$

$$A_3\theta_{r+1} = B_3, \theta_{r+1}(\xi_{\bar{N}}) = 1, \theta_{r+1}(\xi_0) = 0 \quad (37)$$

$$A_4\phi_{r+1} = B_4, \phi_{r+1}(\xi_{\bar{N}}) = 1, \phi_{r+1}(\xi_0) = 0 \quad (38)$$

where,

$$A_1 = D, B_1 = p_r \quad (39)$$

$$A_2 = diag\left(n(-p'_{r+1})^{n-1}\right)D^2 + diag\left(\left(\frac{2mn-m+1}{n+1}\right)f_{r+1}p'_{r+1}\right)$$

$$D - MI, B_2 = mp^2_{r+1} \quad ....(40)$$

$$A_3 = diag(1+Dsp_{r+1})D^2 + diag\left(\Pr\left(\frac{2mn-m+1}{n+1}\right)f_{r+1} + Dsp'_{r+1}\right)$$

$$D - diag\left(r\Pr p_{r+1}\right)I, B_3 = 0 \quad ....(41)$$

$$A_4 = D^2 + diag\left(Sc\left(\frac{2mn-m+1}{n+1}\right)f_{r+1}\right)D - diag\left(rScp_{r+1}\right)I, B_4 = 0$$

...(42)

In equations (39)-(42), *I* is an identity matrix and diag[ ] is a diagonal matrix, all of size $(\bar{N}+1)\times(\bar{N}+1)$ where $\bar{N}$ is the number of grid points, f, p, θ and ϕ are the values of the functions f, p, θ and ϕ, respectively, when evaluated at the grid points and the subscript r denotes the iteration number.

The initial guesses to start the SRM scheme for equations (27)-(32) are chosen as

$$f_0(\eta) = 1-e^{-\eta}, p_0(\eta) = e^{-\eta}, \theta_0(\eta) = e^{-\eta}, \phi_0(\eta) = e^{-\eta} \quad (43)$$

which are randomly chosen functions that satisfy the boundary conditions. The iteration is repeated until convergence is achieved. The convergence of the SRM scheme is defined in terms of the infinity norm as

$$Er = Max\left(\left\|f_{r+1} - f_r\right\|, \left\|p_{r+1} - p_r\right\|, \left\|\theta_{r+1} - \theta_r\right\|, \left\|\varphi_{r+1} - \varphi_r\right\|\right) \quad (44)$$

The convergence rate of the SRM algorithm can be significantly improved by applying the successive over-relaxation (SOR) technique to equations (35)-(38). Under the SOR framework, a convergence controlling relaxation parameter ω is introduced and the SRM scheme for finding, say *X*, is modified to

$$AX_{r+1} = (1-\omega)AX_r + \omega B \quad (45)$$

The results in the next section show that for ω < 1, applying the SOR method improves the efficiency and accuracy of the SRM.

III. VALIDATION OF RESULTS

The accuracy and robustness of the method have been checked by comparing the SRM results and bvp4c results for various values of power law index parameter n, temperature distribution parameter r, magnetic number *M*, Prandtl number *Pr*, thermal dispersion parameter *Ds* and Schmidt number Sc which are given in tabular form in Tables 1 to 4. It is clearly seen that both results are in good agreement. It is relevant to mention here that bvp4c is an in-built ODE solver in Matlab. In order to further establish the accuracy of our numerical computations, we have also compared the values of magnitude of the skin friction coefficient $-f''(0)$ obtained by Andersson et al. [24] and Chen [17], respectively with the respective values calculated by the SRM technique. This comparison is presented in Tables 4 and it has been observed that our

ISSN (Online) 2456 -1304

International Journal of Science, Engineering and Management (IJSEM)
Vol 2, Issue 6, June 2017

results are in full agreement with the results obtained by Andersson et al. [24] and Chen [17].

IV. RESULTS AND DISCUSSION

We have studied steady laminar flow of heat and mass transfer in past a stretching flat sheet in the presence of thermal dispersion. Electrically conducting non-Newtonian power-law fluid has been considered for the present investigation. The nonlinear coupled ordinary differential equations (12)-(14) subject to the boundary conditions (15)-(16) have been solved numerically using spectral relaxation method. We determine through numerical experimentation that $\eta_\infty = 25$ with the grid points $\overline{N} = 100$, give sufficient accuracy for the spectral relaxation method. To determine the convergence, accuracy and general validity of the SRM method, the results were compared with the Matlab bvp4c results for selected values of the governing physical parameters.

With the consideration of the heat transfer analysis on boundary layer flows. As above mentioned analysis, the global self similarity solutions for the non-Newtonian flows $(n \neq 1)$ and heat transfer are valid only when $m = 1/3.$ then we only investigate this case.

Figures 1-3 are the graphical representation of the velocity, temperature and concentration profiles for various values of *M* for different cases of n i.e. shear thinning fluids $(n < 1)$, Newtonian fluid $(n = 1)$, and shear thickening fluids $(n > 1)$. From the figure 1 that the rate of transport is considerably reduced with an increase in *M*. it is clearly indicates that the transverse magnetic field opposes the transport phenomena. This is due to the fact that the variation of magnetic field leads to the variation of Lorentz force, due to magnetic field and the Lorentz force produces resistance to the transport phenomena. These results are consistent with the results of Andersson et al.[24]. Also figure 1 revel that the boundary layer thickness is larger for shear thickening that is dilatant fluids $(n > 1)$ as compared to Newtonian fluid $(n = 1)$ and shear thinning fluids i.e. pseudo-plastic fluids $(n < 1)$. From the figures 2 and 3, it observed that increase in M leads to an increase the temperature and concentration of the fluid. This is due to the face that Loremtz force increases the function between its layers and this is responsible for an increase in the temperature and concentration of the fluid. From these figures we see that the thermal and concentration boundary layer thickness is larger for shear thinning fluids $(n < 1)$ as compared to Newtonian $(n = 1)$ and shear thickening fluids $(n > 1)$. Figures 4 and 5 is graphed for the different values of temperature distribution parameter r on temperature and concentration profiles. From these figures an increase in the values of r is to decrease the thickness of the thermal and concentration boundary layers. In this consistent with the physical situation that the thermal and concentration boundary layer thickness decreases as r increases. Figure 6 shows that the effects of thermal dispersion on temperature profile. From the sketch, an increase in the thermal dispersion effect increases the thermal boundary layer thickness i.e. thermal dispersion enhances the transport of heat along the normal direction to the wall as compared with the case where dispersion is neglected (i.e. *Ds* = 0). In general, this for may be useful in showing that, the use of fluid medium with better heat dispersion properties may be result in better heat transfer characteristics that may be required in many industrial applications (like those concerned with packed bed reactors, nuclear waste disposal, etc.). The variation of generalized Prandtl number Pr on temperature profile is shown in figure 7. As shown in figure 7, the non-dimensional temperature decreases with an increase in Pr for shear thickening fluids $(n > 1)$, Newtonian fluid $(n = 1)$ and shear thinning fluids $(n < 1)$ for $r = -1/2.$ Note that the generalized Prandtl number defined in eqn.() contains in x so that the heat transfer analysis is local. These kinds of results are only valid for large x or small x. The present results are valid for all $x.$ physically, a higher value of Pr is equivalent to decreasing thermal conductivity which reduces conduction and thereby increases the wall heat transfer.The concentration profile verses the Schmidt number *Sc* is depicted in figure 8. As shown in figure 8, the non-dimensional concentration decreases with an increase in *Sc* for shear thickening fluids $(n > 1)$, Newtonian fluid $(n = 1)$ and shear thinning fluids $(n < 1)$ for $r = -1/2.$ Note that the generalized Schmidt number defined in eqn.() contains in x so that the mass transfer analysis is local. These kinds of results are only valid for large x or small $x.$ The present results are valid for all $x.$

Table 1 calculated for the values of derivative of velocity profile i.e. skin-friction coefficient for different values of magnetic field *M* and power law index $n.$ From the table 1, it is observed that skin friction coefficient increases with an raise in *M* values. This is clear indication that the Lorentz force is more effective. The skin-friction coefficient become larger

ISSN (Online) 2456 -1304

International Journal of Science, Engineering and Management (IJSEM)
Vol 2, Issue 6, June 2017

for shear thickening fluids $(n>1)$compared to Newtonian fluid $(n=1)$ and shear thinning fluids $(n<1)$. Table 2 tabulated for different values of M, r, Ds and $\Pr$ for the behavior for the derivative of temperature profile i.e. local Nusselt number. From the date, it is clear that hear transfer rate decreases with an increase in M & Ds. Furthermore heat transfer rate increases with an increase in r & $\Pr$. The rate of heat transfer become larger for shear thinning fluids $(n<1)$ compared to Newtonian fluid $(n=1)$and shear thickening fluids $(n>1)$. Table 3 contains the derivative for concentration profile that also gives the behavior of local Sherwood number Sh_x for different values of n, M, r & Sc. From the data in table 3, it is observed that with the increase in r & Sc, local Sherwood number increases, while increase in Schmidt number Sc, decrease the local Sherwood number. The rate of mass transfer become larger for shear thinning fluids $(n<1)$ compared to Newtonian fluid $(n=1)$and shear thickening fluids $(n>1)$.

V.CONCLUSIONS

In this study we have presented the laminar boundary layer flow of heat and mass transfer in magnetohydrodynamic non-Newtonian power-law fluid over stretching flat sheet in the presence of thermal dispersion. The main results of present analysis are listed below

- The momentum boundary layer thickness is larger for shear thickening that as compared to Newtonian fluid and shear thinning fluids.
- The thermal and concentration boundary layer thickness is larger for shear thinning fluids as compared to Newtonian fluid and shear thickening fluids.
- The thermal dispersion parameter has a strong influence over the temperature profiles.
- The skin-friction coefficient become larger for shear thickening fluids compared to Newtonian fluid and shear thinning fluids.
- The rate of heat and mass transfer become larger for shear thinning fluids compared to Newtonian fluid and shear thickening fluids.

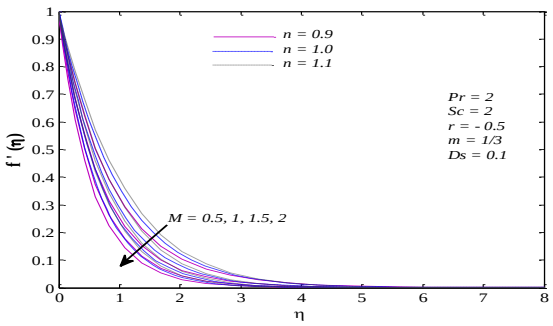

Figure 1: Graph of SRM solutions for velocity profile $f'(\eta)$ for different values of M

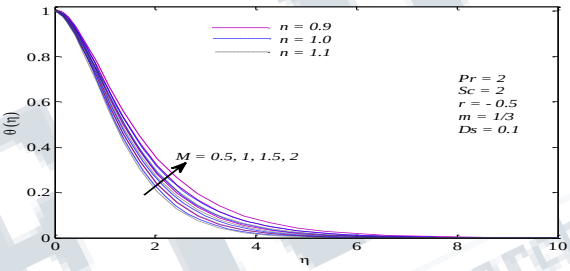

Figure 2: Graph of SRM solutions for temperature profile $\theta(\eta)$ for different values of M

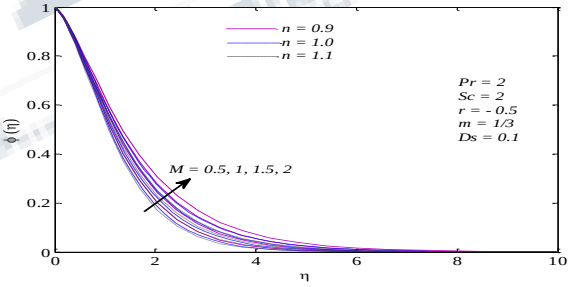

Figure 3: Graph of SRM solutions for concentration profile $\phi(\eta)$ for different values of M

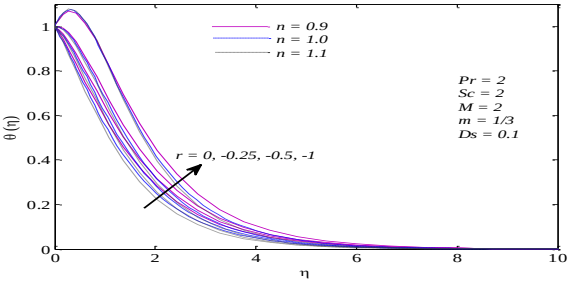

ISSN (Online) 2456 -1304

International Journal of Science, Engineering and Management (IJSEM)
Vol 2, Issue 6, June 2017

Figure 4: Graph of SRM solutions for temperature profile $\theta(\eta)$ for different values of r

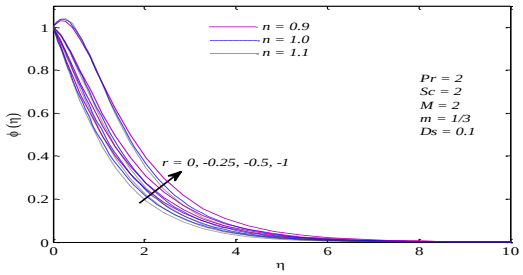

Figure 5: Graph of SRM solutions for concentration profile $\phi(\eta)$ for different values of r

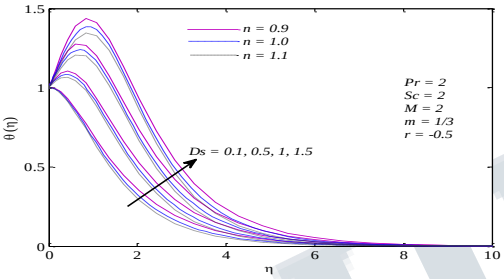

Figure 6: Graph of SRM solutions for temperature profile $\theta(\eta)$ for different values of Ds

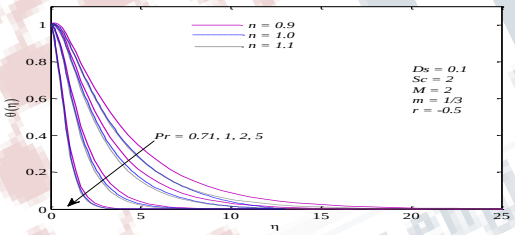

Figure 7: Graph of SRM solutions for temperature profile $\theta(\eta)$ for different values of $\Pr$

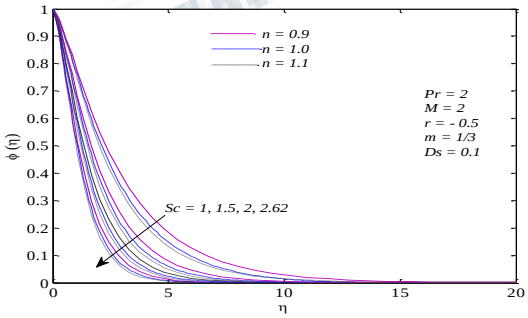

Figure 8: Graph of SRM solutions for concentration profile $\phi(\eta)$ for different values of Sc

Table 1 Numerical values for $\mathrm{Re}_x^{1/(n+1)} C_f$ at the surface for different values of $n \& M$ with $\Pr = Sc = 3, r = -1/2, m = 1/3 \& Ds = 0.5.$

M	n	$\mathrm{Re}_x^{1/(n+1)} C_f$			
		Iter	Basic SRM	SRM with SOR	Bvp4c
0.5	0.9	76	2.08287314	2.08287314	2.08287314
1.0		16	2.55502216	2.55502216	2.55502216
1.5		16	2.94630671	2.94630671	2.94630671
2.0		16	3.28711657	3.28711657	3.28711657
0.5	1.0	16	1.95067816	1.95067816	1.95067816
1.0		14	2.40737345	2.40737345	2.40737345
1.5		12	2.79120161	2.79120161	2.79120161
2.0		11	3.12859271	3.12859271	3.12859271
0.5	1.1	100	1.65806074	1.65806074	1.65806074
1.0		81	2.05866785	2.05866785	2.05866785
1.5		21	2.39935573	2.39935573	2.39935573
2.0		23	2.70117279	2.70117279	2.70117279

Table 2 Numerical values for $-\theta'(0)$ at the surface for $n, M, r, Ds \& \Pr$ for Sc =2

M	r	Ds	Pr	n	Iter	$-\theta'(0)$		
						Basic SRM	SRM with SOR	Bvp4c
0.5	-0.5	0.1	2	0.9	76	0.06058048	0.06058048	0.06058048
1.0					16	0.01786960	0.01786960	0.01786960
1.5					16	-0.01573138	-0.01573138	-0.01573138
2					16	-0.04383736	-0.04383736	-0.04383736
2	0.0				16	0.32719448	0.32719448	0.32719448
	-0.25				16	0.14999730	0.14999730	0.14999730
	-0.5				16	-0.04383736	-0.04383736	-0.04383736
	-1.0				16	-0.49733460	-0.49733460	-0.49733460
	-0.5	0.3			16	-0.31175884	-0.31175884	-0.31175884
		0.5			16	-0.47916878	-0.47916878	-0.47916878
		1.0			16	-0.68733155	-0.68733155	-0.68733155
		1.5			16	-0.76750198	-0.76750198	-0.76750198
		0.1	0.71		16	-0.11387843	-0.11387843	-0.11387843
			1.0		16	-0.09696820	-0.09696820	-0.09696820
			2.0		16	-0.04383736	-0.04383736	-0.04383736
			5.0		16	0.08571821	0.08571821	0.08571821
0.5				1.0	16	0.08011287	0.08011287	0.08011287
1.0					14	0.04312578	0.04312578	0.04312578
1.5					12	0.01404599	0.01404599	0.01404599
2					11	-0.01017553	-0.01017553	-0.01017553
2	0.0				11	0.38547127	0.38547127	0.38547127
	-0.25				11	0.19771171	0.19771171	0.19771171
	-0.5				11	-0.01017553	-0.01017553	-0.01017553
	-1.0				11	-0.50891619	-0.50891619	-0.50891619
	-0.5	0.3			11	-0.24986407	-0.24986407	-0.24986407
		0.5			11	-0.40032226	-0.40032226	-0.40032226
		1.0			11	-0.58775568	-0.58775568	-0.58775568
		1.5			11	-0.65922893	-0.65922893	-0.65922893
		0.1	0.71		11	-0.07904313	-0.07904313	-0.07904313
			1.0		11	-0.06533856	-0.06533856	-0.06533856
			2.0		11	-0.01017553	-0.01017553	-0.01017553
			5.0		11	0.12676255	0.12676255	0.12676255
0.5				1.1	100	0.09436713	0.09436713	0.09436713
1.0					81	0.06155459	0.06155459	0.06155459
1.5					23	0.03574581	0.03574581	0.03574581
2					23	0.01426926	0.01426926	0.01426926
2	0.0				23	0.42871886	0.42871886	0.42871886
	-0.25				23	0.23305925	0.23305925	0.23305925
	-0.5				23	0.01426926	0.01426926	0.01426926
	-1.0				23	-0.52200996	-0.52200996	-0.52200996
	-0.5	0.3			23	-0.20609181	-0.20609181	-0.20609181
		0.5			23	-0.34509173	-0.34509173	-0.34509173
		1.0			23	-0.51878835	-0.51878835	-0.51878835
		1.5			23	-0.58458140	-0.58458140	-0.58458140
		0.1	0.71		23	-0.06570196	-0.06570196	-0.06570196
			1.0		23	-0.04615631	-0.04615631	-0.04615631
			2.0		23	0.01426926	0.01426926	0.01426926
			5.0		23	0.15687263	0.15687263	0.15687263

ISSN (Online) 2456 -1304

International Journal of Science, Engineering and Management (IJSEM)
Vol 2, Issue 6, June 2017

Table 3 Numerical values for at the surface for for Ds = 0.1, Pr = 2.

M	r	Sc	n	Iter	$-\phi'(0)$		
					Basic SRM	SRM with SOR	Bvp4c
0.5	-0.5	2	0.9	76	0.19771950	0.19771950	0.19771950
1.0				16	0.17767767	0.17767767	0.17767767
1.5				16	0.16280138	0.16280138	0.16280138
2				16	0.15112308	0.15112308	0.15112308
2	0				0.54909447	0.54909447	0.54909447
	-0.25				0.35935001	0.35935001	0.35935001
	-0.5				0.15112308	0.15112308	0.15112308
	-1.0				-0.33920018	-0.33920018	-0.33920018
	-0.5	0.24		16	0.02178220	0.02178220	0.02178220
		0.62		14	0.05367139	0.05367139	0.05367139
		0.78		12	0.06630382	0.06630382	0.06630382
		2.68		11	0.18845038	0.18845038	0.18845038
0.5			1.0	11	0.20666515	0.20666515	0.20666515
1.0				11	0.18837817	0.18837817	0.18837817
1.5					0.17449405	0.17449405	0.17449405
2					0.16342655	0.16342655	0.16342655
2	0			100	0.58603553	0.58603553	0.58603553
	-0.25			81	0.38582167	0.38582167	0.38582167
	-0.5			23	0.16342655	0.16342655	0.16342655
	-1.0			23	-0.37379829	-0.37379829	-0.37379829
	-0.5	0.24		23	0.06275782	0.06275782	0.06275782
		0.62		23	0.06918295	0.06918295	0.06918295
		0.78		23	0.07812924	0.07812924	0.07812924
		2.68		23	0.20268224	0.20268224	0.20268224
0.5			1.1	23	0.21332033	0.21332033	0.21332033
1.0					0.19654951	0.19654951	0.19654951
1.5					0.18360649	0.18360649	0.18360649
2					0.17313461	0.17313461	0.17313461
2	0				0.61432653	0.61432653	0.61432653
	-0.25				0.40639008	0.40639008	0.40639008
	-0.5				0.17313461	0.17313461	0.17313461
	-1.0				-0.40265394	-0.40265394	-0.40265394
	-0.5	0.24			0.02600779	0.02600779	0.02600779
		0.62			0.06337832	0.06337832	0.06337832
		0.78			0.07795525	0.07795525	0.07795525
		2.68			0.21382983	0.21382983	0.21382983

Table 4 Comparison of Skin-friction coefficient $-f''(0)$ with the available results in literature for different values of M when $\Pr = Sc = Ds = 0, r = -0.5, m = n = 1.$.

M	$-f''(0)$		
	Present study	Chen [17]	Andersson et al.[24]
0.0	1.000000	1.00000	1.000
0.5	1.224745	1.22475	1.225
1.0	1.414214	1.41421	1.414
1.5	1.581139	1.58114	1.581
2.0	1.732051	1.73205	1.732

REFERENCES

1. Sakiadis B.C., (1961), Boundary-layer behavior on continuous solid surfaces: I. Boundary-layer equations for two-dimensional and axisymmetric flow, AIChE Journal, Vol. 7, pp.26-28.

2. Tsou F. K., Sparrow E.M., Glodstein R.J., (1967), Flow and heat transfer in the boundary layer on a continuous moving surface, Inter National Journal of Heat and Mass Transfer, Vol.10, pp. 219-235.

3. Erickson L.E., Fan L.T., Fox V.G., (1966), Heat and mass transfer on a moving continuous flat plate with suction or injection, Journal of Industrial and Engineering Chemistry, Vol.5, pp.19-25.

4. Ishak A., (2010), Thermal boundary layer flow over a stretching sheet in a micropolar fluid with radiation effect, Meccanica, Vol.45, pp.367–373.

5. Ishak A., Nazar R., and Pop I., (2009), Boundary layer flow and heat transfer over an unsteady stretching vertical surface, Meccanica, Vol.44, pp.369–375.

8. Xu H., Jun Liao S., (2009), Laminar flow and heat transfer in the boundary-layer of non-Newtonian fluids over a stretching flat sheet, Computers and Mathematics with Applications, Vol.57, pp.1425-1431.

9. Hassanien I.A., Abdullah A.A., Gorla R.S.R., (1998), Flow and Heat Transfer in a Power-Law Fluid over a Non-isothermal Stretching Sheet, Mathl. Comput. Modelling, Vol. 28, No. 9, pp. 105-116.

10. Mahmoud M. A. A. and Megahed A. M., (2009), Effects of viscous dissipation and heat generation (absorption) in a thermal boundary layer of a non-Newtonian fluid over a continuously moving permeable flat plate, Journal of Applied Mechanics and Technical Physics, Vol. 50, No. 5, pp. 819–825.